Solvent Recovery Targeting

Berit S. Ahmad and Paul I. Barton
Dept. of Chemical Engineering and Energy Laboratory, Massachusetts Institute of Technology, Cambridge, MA 02139

One of the environmental challenges faced by the pharmaceutical and specialty chemical industries is the widespread use of organic solvents. With a solvent-based chemistry, the solvent necessarily has to be separated from the product. Chemical species in waste-solvent streams typically form multicomponent azeotropic mixtures, and this often complicates separation and, hence, recovery of solvents. A design approach is presented whereby process modifications proposed by the engineer to reduce the formation of waste-solvent streams can be evaluated systematically. This approach, called solvent recovery targeting, exploits a recently developed algorithm for elucidating the separation alternatives achievable when applying batch distillation to homogeneous multicomponent mixtures. The approach places the composition of the waste-solvent mixture correctly in the relevant residue curve map and computes the maximum amount of pure material that can be recovered via batch distillation. Solvent recovery targeting is applied to two case studies derived from real industrial processes.

Introduction

Increasingly aggressive legislation and growing concern over environmental impacts are motivating the chemical manufacturing industry to reassess their current operations. The traditional approach has been to employ ever more sophisticated end-of-pipe treatment technologies. More recently, the more forward looking policy of pollution prevention has been adopted: defined by the U.S. Environmental Protection Agency as ''the use of materials, processes, or practices that reduce or eliminate the creation of pollutants or waste at the source'' (Freeman et al., 1992). Experience indicates that, on average, about 80% of emissions from chemical facilities are generated by 20% of the sources (Chadha and Parmele, 1993). It is therefore important to identify and focus on the major contributors.

One of the many challenges faced by the pharmaceutical and specialty chemical industries is the widespread use of organic solvents. Solvents are used in a broad spectrum of unit operations ranging from reaction and separation to product washing and equipment cleaning. Many solvents are being phased out of products and processes for environmental and health reasons (Kirschner, 1994). For example, cleaning solvents are relatively easy to change or eliminate (Heckman, 1991). On the other hand, solvents in process reactions are much more difficult to substitute, because most process solvents influence the character of the reaction product (Kirschner, 1994). With a solvent-based chemistry, the solvent necessarily has to be separated from the product stream. Although intermediate storage may be required before the solvent can be recycled to subsequent batches, this should be preferred to disposal of the solvent as toxic waste.

Chemical species in waste-solvent streams generated by these industries typically form multicomponent azeotropic mixtures. This highly nonideal behavior often complicates separation and, hence, recovery of the solvents. The pollution-prevention strategy developed in this article is based on understanding and mitigating such obstacles. A simple batch process consisting of a reactor and a rectifier is presented in Figure 1 to illustrate the procedure. Although simple, the problems encountered in this flowsheet are representative of the class of processes studied in this work. Component R reacts to form product P and byproduct BP. R is exhausted by the reaction, BP is undesired and is treated as organic waste, while it is desirable to recover and recycle the solvent S. The feasibility of distilling the ternary mixture P, BP, and S can be determined from a study of the relevant ternary *residue curve map* (see Figure 1b). S and BP form a maximum boiling binary azeotrope S-BP. As a consequence, only one of the species S and BP can be recovered in pure form.

Correspondence concerning this article should be addressed to P. I. Barton.
Current address of B. S. Ahmad: Norsk Hydro ASA, P.O. Box 200, N-1321, Stabekk, Norway.

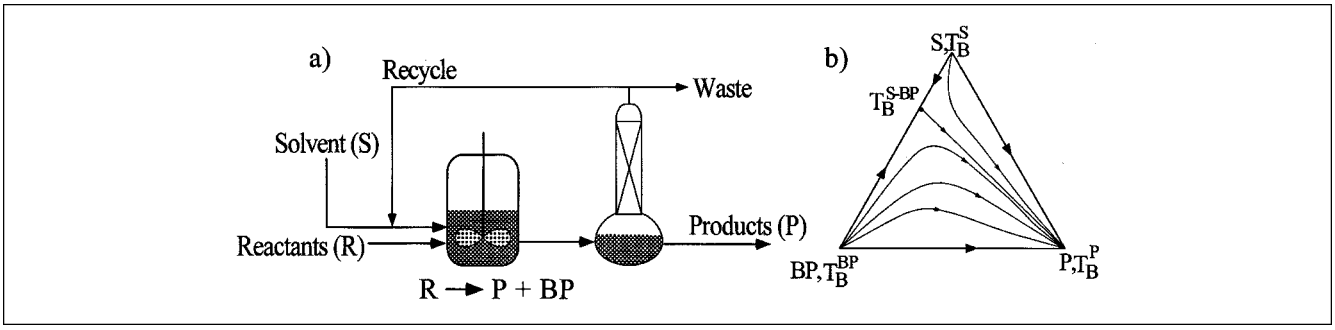

Figure 1. (a) Simple process consisting of a reaction task and a separation task; (b) residue curve map for the mixture leaving the reactor.

The two possible distillation sequences are (1) $S \rightarrow S\text{-}BP \rightarrow P$; (2) $BP \rightarrow S\text{-}BP \rightarrow P$, depending on the initial composition in the reboiler. If alternative 1 is chosen, pure *S* is recovered and can be recycled to the subsequent batch. However, the binary azeotrope *S-BP* will have to be disposed of, as it is the only means by which *BP* can be removed from the system. Hence, extra solvent has to be added to the process with every batch, and subsequently disposed. On the other hand, alternative 2 will result in recovery of nearly pure *BP*, which is also subject to disposal, while the binary azeotrope can be recycled to the subsequent batch. Alternative 2 obviously provides environmental benefits over alternative 1, because nearly all of the solvent is recovered and recycled. Some organic waste (*BP*) is generated, but this is a result of the stoichiometry and is unavoidable without altering the chemistry. In conclusion, this analysis has revealed that the final reaction mixture should ideally have a composition that is located in the region bounded by *BP*, *S-BP*, and *P*. This can be achieved in principle by adjusting the amount of solvent added to the reactor during startup before cyclic steady state is reached. Before implementation in plant, the impact of recycling *BP* through the *S-BP* azeotrope on the reaction kinetics must also be analyzed.

As demonstrated in the above example, the sequence of pure component and azeotropic cuts generated by batch distillation of a multicomponent azeotropic mixture, and the maximum feasible recovery in each cut, is highly dependent on the initial composition of the mixture. Any species that is recovered in azeotropic cuts that cannot be recycled is likely to leave the process and be treated as toxic waste. The ability to predict the feasibility of recovering components in pure form from a process stream is therefore essential to pollution prevention in these manufacturing systems. This work presents a rapid and automated approach to generating this prediction, assuming that batch distillation is the separation technology employed. The use of batch distillation as a multipurpose separation operation is typical in the industries concerned, and economics and simplicity of control make batch distillation one of the most attractive methods for solvent recovery (Hassan and Timberlake, 1992).

The approaches currently available to obtain such predictions, such as, test runs in pilot plants or detailed dynamic simulation studies are typically very elaborate and time consuming. On the other hand, Van Dongen and Doherty (1985) show that the desired information can be readily extracted from the residue curve map that is characteristic of *simple distillation.* Ahmad and Barton (1996) extend and generalize the theory for ternary and quaternary residue curve maps to *systems with an arbitrary number of components.* These theoretical results prompt us to develop systematic and general tools for the design of batch processes with minimum waste.

In this article, the algorithm for characterizing the batch distillation composition simplex for a system with an arbitrary number of components developed by Ahmad et al. (1998) is exploited in a sequential design strategy where process streams or mixed waste-solvent streams are analyzed for maximum feasible solvent recovery using a targeting approach. This procedure is termed *solvent recovery targeting.* Solvent recovery targeting yields an understanding of the barriers to solvent recovery created by a particular design, such as the existence of a particular azeotrope in solvent mixtures. This information can then be used to modify the design, aiming at enhanced solvent recovery and recycling.

Approach

For a given base case, solvent recovery targeting, given the composition of the mixture(s) to be separated, will predict the correct distillation sequence and calculate the maximum feasible recovery of each product cut in the sequence. It can further provide information about all other feasible distillation sequences involving the same set of pure components. This information is used to evaluate the feasibility of enhancing solvent recovery in the proposed flowsheet. If necessary, the original design is modified, and the targeting approach is next applied to the new process streams to evaluate the modifications. The general structure of solvent recovery targeting is outlined in Figure 2. Analyzing the stream for maximum recovery involves two tasks: (1) locating the stream composition in the correct batch distillation region; and (2) calculating the amounts recovered in each product cut. In the subsequent sections the different steps are described.

Local Initial Composition

Ahmad and Barton (1996) explore the structure imposed on the composition simplex (residue curve map) of a homogeneous multicomponent system describing batch distillation by the presence of azeotropes. This structure can be visualized by dividing the simplex (regular simplex) into a series of dis-

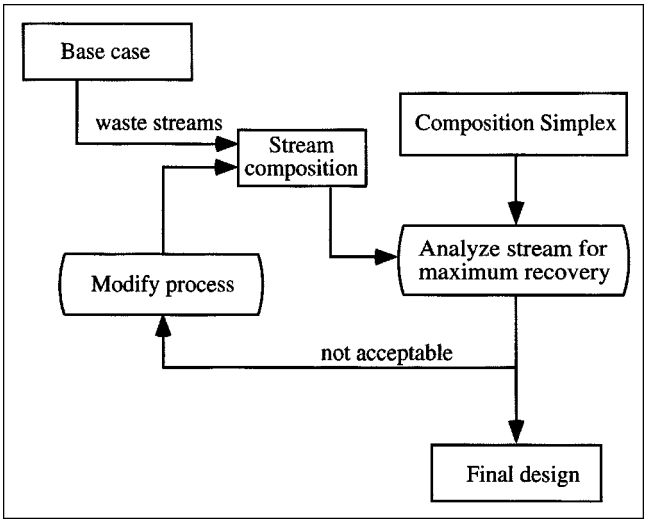

Figure 2. Solvent recovery targeting.

tinct batch distillation regions. All initial compositions within a particular batch distillation region will result in the same sequence of product cuts, and these cuts will have compositions close to pure components or azeotropes. Each batch distillation can therefore be characterized by a product simplex. The product simplex is also a regular simplex with the same dimensions as the composition simplex itself.

Let B represent a batch distillation region for an *nc* component mixture, while $\mathbf{\Pi}^{nc}$ refers to the corresponding product simplex formed from *nc* fixed points. $\mathbf{\Pi}^{nc}$ is a $(nc-1)$-geometric simplex and defined by Eq. 1.

$$\mathbf{\Pi}^{nc} = \left\{ x \in R^{nc}: x = \sum_{k=0}^{nc-1} f_k p_k;\ f_k \geq 0\ \forall k = 0, \ldots, nc-1 \text{ and } \sum_{k=0}^{nc-1} f_k = 1 \right\} \quad (1)$$

where $f_k\ \forall k = 0, \ldots, nc-1$ are barycentric coordinates. The element p_{ki} represents the molefraction of pure component *i* in product cut *k* in the *nc* vector p_k.

Let $P = \{p_0, p_1, \ldots, p_{nc-1}\}$ represent the sequence of product cuts resulting from any composition located in batch distillation region B. From the definition of batch distillation regions (Ahmad and Barton, 1996), it follows that if the initial composition of interest ($x^{p,0}$) is located in batch distillation region B, it must also be located in product simplex $\mathbf{\Pi}^{nc}$ formed from the *nc* fixed points in *P*. Hence, it is necessary that $x^{p,0}$ satisfies Eq. 2 with respect to $\mathbf{\Pi}^{nc}$:

$$x = \sum_{k=0}^{nc-1} f_k p_k;\ f_k \geq 0\ \forall k = 0, \ldots, nc-1 \quad \text{and} \quad \sum_{k=0}^{nc-1} f_k = 1 \quad (2)$$

Physically, the scalars f_k represent the fractions of $x^{p,0}$ that will be recovered in each product cut using batch distillation under the limiting conditions. The fact that both $x^{p,0}$ and the set of points $\{p_k\ \forall k = 0, \ldots, nc-1\}$ lie in the hyperplane $\sum_{i=1}^{nc} x_i = 1$ implies that the criterion $\sum_{k=0}^{nc-1} f_k = 1$ is satisfied. If one or more $f_k = 0$, this implies that $x^{p,0}$ lies on one of the faces of $\mathbf{\Pi}^{nc}$.

Any composition in the composition space will yield a unique product sequence. However, since the batch distillation regions fill the composition simplex, and a product simplex will either coincide or be larger than its batch distillation region, two or more product simplices can possibly intersect. In that case, two or more product sequences will satisfy Eq. 2 for the same initial composition. In general, applying Eq. 2 to initial composition $x^{p,0}$ may yield three different outcomes depending on the location of $x^{p,0}$:

(1) One of the product sequences satisfies Eq. 2. Hence, there is only one positive product simplex, and, consequently, the correct product sequence is found.

(2) More than one product sequence satisfies Eq. 2, and the product sequences found will produce the same unstable node in the first cut.

(3) More than one product sequence satisfies Eq. 2, and the product sequences found will give us rise to different unstable nodes in the first cut.

To illustrate the possible outcomes, consider the ternary system in Figure 3a. The system has four batch distillation regions and therefore four product sequences, represented by $P_1 = \{\text{m1, n1, n3}\}$, $P_2 = \{\text{m1, n2, q1}\}$, $P_3 = \{\text{m2, n2, q1}\}$, and $P_4 = \{\text{m2, n3, q1}\}$. P_1 and P_2 have the unstable node m1 in common, while P_3 and P_4 have m2 in common. Product simplex $\mathbf{\Pi}_1^3$ intersects product simplices $\mathbf{\Pi}_2^3$, $\mathbf{\Pi}_3^3$, and $\mathbf{\Pi}_4^3$. The intersections are represented by the domains 2a, 3a, and 4a, respectively. If $x^{p,0}$ is located in domains 1, 2b, 3b, or 4b, outcome 1 above will result, if $x^{p,0}$ is located in domain 2a outcome 2 above will result, and if $x^{p,0}$ is located in domains 3a or 4a outcome 3 will result. If outcome 2 or 3 is encountered, further examination is required in order to determine the correct product sequence.

Product sequences that have an unstable node in common

Consider the ternary system in Figure 4. The system has four batch distillation regions (see Figure 4b). Hence, four product simplices can be generated, defined by $\mathbf{\Pi}_1^3{:}P_1 = \{\text{m1,n1,n3}\}$, $\mathbf{\Pi}_2^3{:}P_2 = \{\text{m1,n4,q1}\}$, $\mathbf{\Pi}_3^3{:}P_3 = \{\text{m1,n3,n4}\}$, and $\mathbf{\Pi}_4^3{:}P_4 = \{\text{m1,n2,n4}\}$ as indicated in Figure 4c. They all have the unstable node m1 in common. One of the facets of $\mathbf{\Pi}_3^3$ intersects the stable separatrix connecting the binary azeotrope n4 and the ternary azeotrope at the point *t*. The composition simplex can therefore be divided into five domains (see Figure 4d). When applying Eqs. 2, five possible scenarios can take place depending on the location of the initial composition. The different scenarios are summarized in Table 1.

Correct prediction of the true product sequence can be confirmed by placing $x^{p,0}$ anywhere in the composition space, and then drawing a straight line through $x^{p,0}$ and m1. The pot composition path will move along this line away from m1 until it encounters a *pot composition boundary* [see Ahmad and Barton (1996)]. In scenario 3 the pot composition path intersects the pot composition boundary connecting n4 and

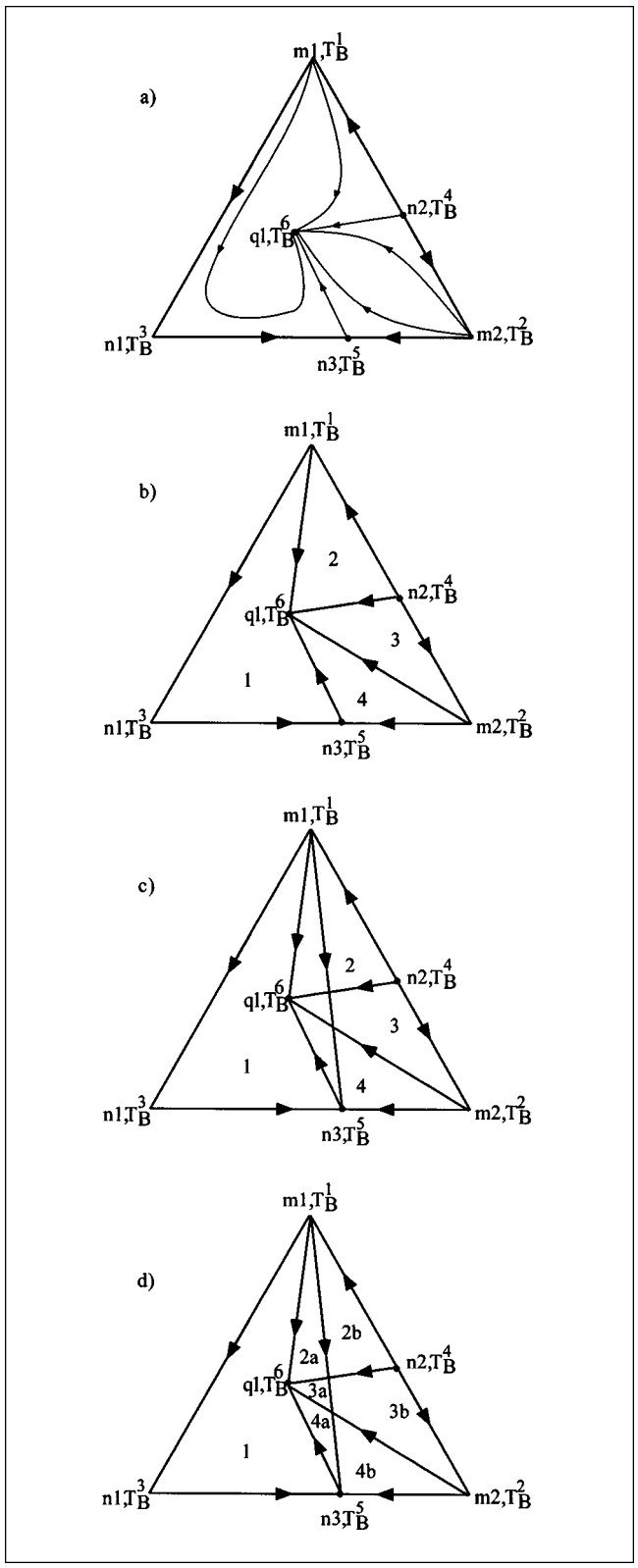

Figure 3. Ternary system with intersecting product simplices.

(a) Simple distillation residue curve map; (b) batch distillation regions; (c) product simplices; (d) intersecting domains.

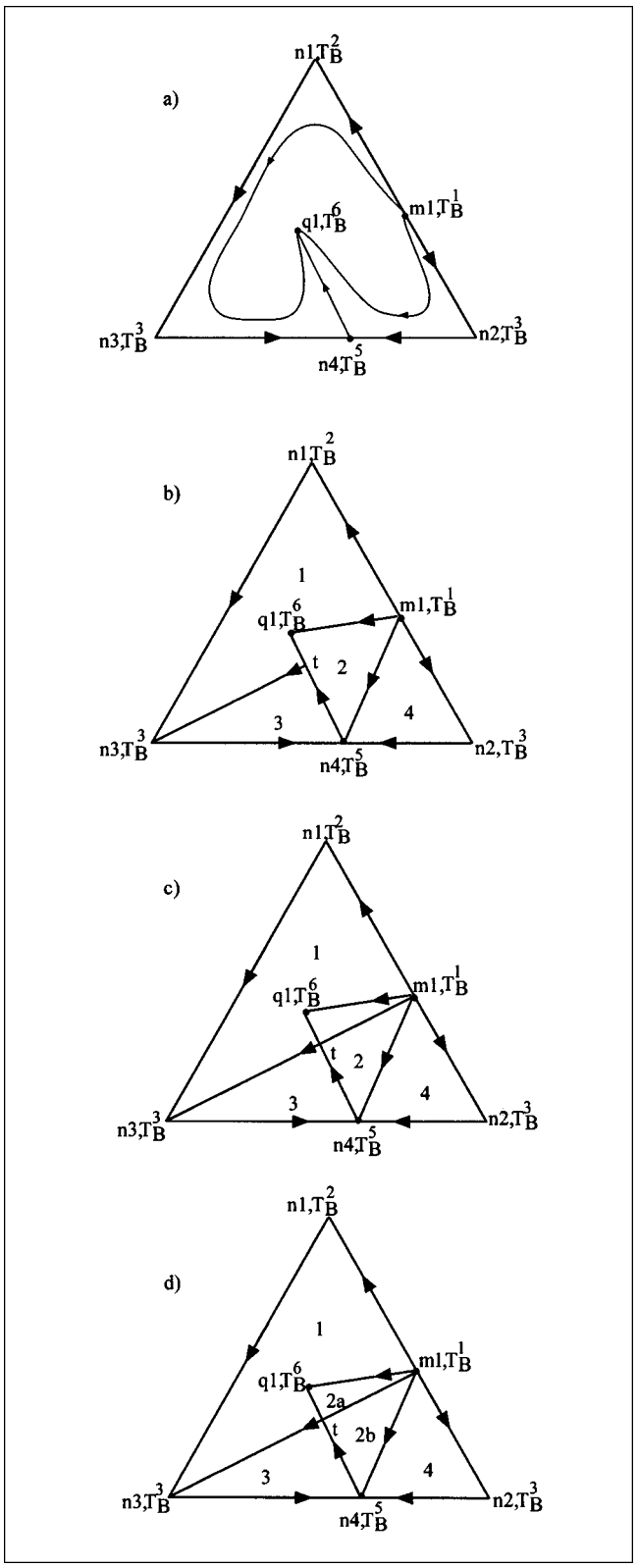

Figure 4. Ternary system with intersecting product simplices.

(a) Simple distillation residue curve map; (b) batch distillation regions; (c) product simplices; (d) intersecting domains.

Table 1. Possible Scenarios When Testing for Positive Barycentric Coordinates

Case	Location of $x^{p,0}$	Positive Product Simplex	True Product Sequence
1	B_1	$\mathbf{\Pi}_1^3$	P_1
2	B_{2a}	$\mathbf{\Pi}_1^3$, $\mathbf{\Pi}_2^3$	P_2
3	B_{2b}	$\mathbf{\Pi}_2^3$, $\mathbf{\Pi}_3^3$	P_2
4	B_3	$\mathbf{\Pi}_3^3$	P_3
5	B_4	$\mathbf{\Pi}_4^3$	P_4

q1, as illustrated by Figure 5. The point of intersection is x^{1a}. Further, the line can be extended until it intersects the pot composition boundary connecting n3 and n4 at x^{1b}. The true product sequence is the set of fixed points P resulting from the batch distillation region that contains the *active pot composition boundary*, defined as the pot composition boundary that is encountered first. *Product simplex boundary* $\hat{\mathbf{\Pi}}^{nc-1}$ of product simplex $\mathbf{\Pi}^{nc}$ is the facet opposite the unstable node p_0, and will be used to approximate the pot composition boundary, in the same manner product simplices are used to approximate batch distillation regions. $\hat{\mathbf{\Pi}}^{nc-1}$ is defined by $nc-1$ vectors formed from the $nc-1$ fixed points that remain when the unstable node is removed from P. Since it is assumed that the pot composition boundary is linear, that is, either located on a facet, or on a stable dividing boundary and the fixed points located on the pot composition boundary lie on a hyperplane, this approximation is an accurate representation of the actual distance. Obviously, if the number of fixed points located on the pot composition boundary is equal to $nc-1$, the pot composition boundary is linear and equal to the corresponding product simplex boundary. In the case that the number of fixed points on the pot composition boundary is greater than $nc-1$, the approximation may result in an overestimation of the distance. This is because the product simplex either coincides or is greater than its corresponding batch distillation region. However, an overestimation of the distance implies that the pot composition

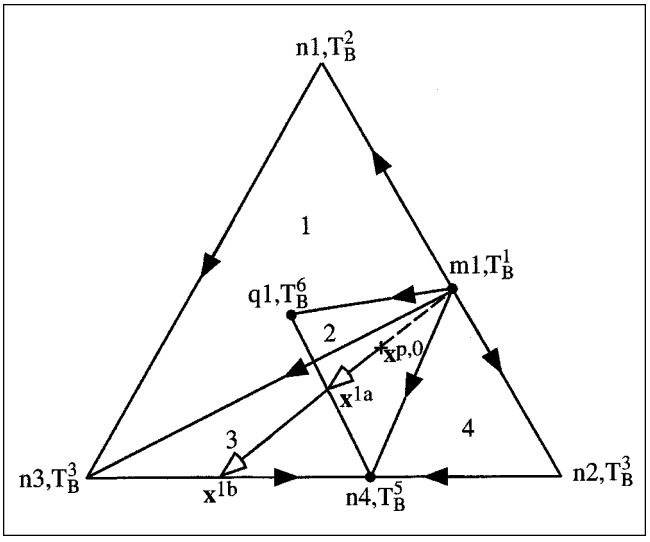

Figure 5. True product sequence is determined by the active pot composition boundary.

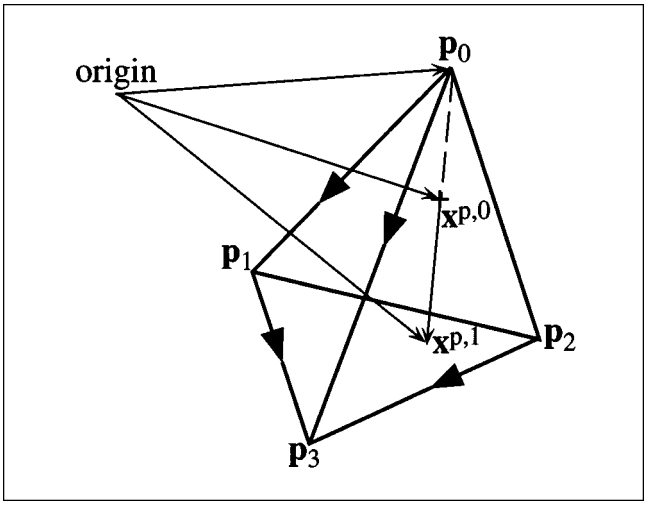

Figure 6. Identification of active product simplex boundary.

boundary is smaller than its corresponding product simplex boundary, and, hence, the batch distillation region is smaller than its corresponding product simplex. Therefore, it is not the active batch distillation region.

Figure 6 shows a product simplex for a quaternary mixture projected into R^2. The relation to the origin ($x=(0, 0, 0, 0)^T$) is indicated for clarity. The initial composition is defined by

$$x^{p,0} = f_0 p_0 + \sum_{k=1}^{nc-1} f_k p_k = f_0 p_0 + (1-f_0) x^{p,1} \qquad (3)$$

where $f_k \ \forall k \in \{0, \ldots, nc-1\}$ are the barycentric coordinates from Eq. 2.

The intersection with the product simplex boundary (defined by p_1, p_2, and p_3) at $x^{p,1}$ can be expressed in terms of the relative distance α, the number of times we need to take the vector $(x^{p,0} - p_0)$ in order to get from p_0 to $x^{p,1}$.

$$x^{p,1} = p_0 + \alpha\left(x^{p,0} - p_0\right) \qquad (4)$$

Combining Eqs. 3 and 4 results in a simple relationship between α and f_0

$$\alpha = \frac{1}{1-f_0} \qquad (5)$$

Hence, the relative distance to the product simplex boundary can be measured in terms of the barycentric coordinate f_0 for the first product cut. The larger α is the further away from the initial composition is $x^{p,1}$. In order to determine the true product sequence, it is therefore sufficient to compare the barycentric coordinates f_0^s for the positive product simplices. The true product simplex is thus $\mathbf{\Pi}^{nc}$ for which

$$f_0^* = \min\{ f_0^s \ \forall s \in \{\text{positive product simplices}\}\} \qquad (6)$$

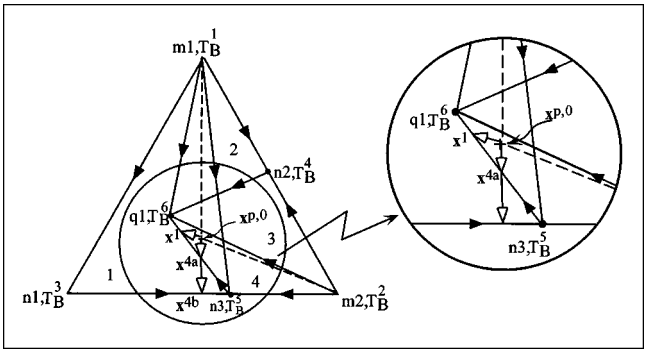

Figure 7. Identification of true product sequence.

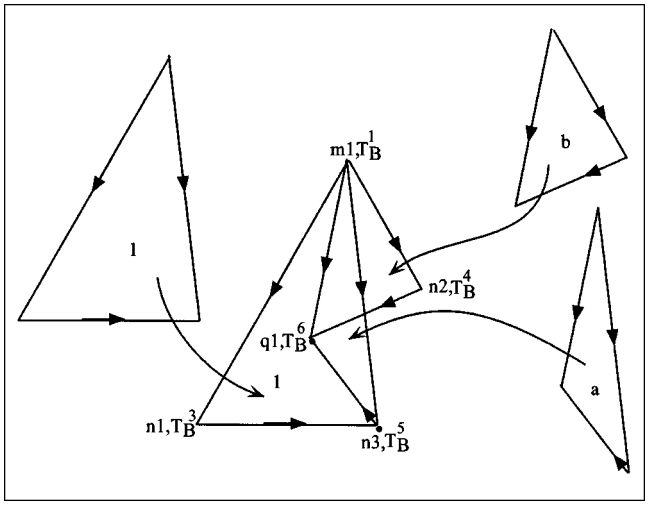

Figure 8. Construction of additional simplices.

If Eq. 6 does not give a unique minimum such as, $f_*^s = f_0^s$ $\forall s \in \{\text{positive product simplices}\}$, then either the product simplex boundaries for the positive product simplices are located on the same facet, or on the stable dividing boundary and the stable dividing boundary is linear (that is, the fixed points in the common unstable boundary limit set are located on a hyperplane). In either case, the product simplex boundaries intersect, in the same manner product simplices may intersect. In order to determine the true product sequence, Eq. 6 has to be replaced by replacing f_0^s with f_1^s and so on, until a unique sequence is found.

Product sequences that do not have an unstable node in common

Clearly, this behavior can be observed only in a system with two or more unstable nodes, and, hence, a stable dividing boundary. The correct product sequence is the one for which the unstable node lies on the same side of the stable dividing boundary as the initial composition. Consider Figure 7. The stable dividing boundary is composed of the straight lines between n3 and q1 and n2 and q1.

Both product simplices 1 and 4 will generate positive barycentric coordinates when applying Eqs. 2 to the initial composition $x^{p,0}$, although $x^{p,0}$ is truly located in batch distillation region 4. The correct product sequence can be determined by drawing straight lines through $x^{p,0}$ and each of the unstable nodes, and extending these lines until they intersect the respective pot composition boundaries of batch distillation regions 1 and 4 (x^1 and x^{4b}). The line from $x^{p,0}$ to the intersection represents the path the pot composition orbit would travel during distillation of the first product cut (with composition equal to the relevant unstable node). Observe that the line from $x^{p,0}$ to x^{4b} also intersects the line connecting n3 and q1, which is part of the stable dividing boundary, at x^{4a}. The path from $x^{p,0}$ to x^{4b} is therefore infeasible, and $x^{p,0}$ cannot give rise to sequence {m1,n1,n3}.

Figure 8 shows product simplex 1 and the stable dividing boundary extracted from Figure 7. The stable dividing boundary can be divided into two pot composition boundaries, approximated by product simplex boundaries $\hat{\mathbf{\Pi}}_a^2 : \hat{P}_a =$ {n2,q1}, and $\hat{\mathbf{\Pi}}_b^2 : \hat{P}_b =$ {n3,q1}. Also note that two 2-simplices (a and b) have been constructed by adding the unstable node m1 to the sets $\hat{P}_a$ and $\hat{P}_b$. We can therefore find the relative distance (α_{sdb}) (see Figure 9), the number of times we need to take the vector ($x^{p,0} - \text{m1}$) in order to get from $x^{p,0}$ to the stable dividing boundary simply by computing the barycentric coordinates for the two simplices with respect to $x^{p,0}$ and applying Eq. 5. The relative distance from $x^{p,0}$ to the pot composition boundary in batch distillation region 1 (α_{ppb}), which is approximated by the product simplex boundary formed by $\hat{P} =$ {n1,n3}, can be computed in a similar manner. If the relative distance from $x^{p,0}$ to the stable dividing boundary is smaller than the distance to the pot composition boundary in batch distillation region 1, the path from the initial composition to the pot composition boundary will intersect the stable dividing boundary. Since $x^{p,0}$ is located in simplex a and in product simplex 1, f_0 computed for simplex b will be negative. It is, therefore, not necessary to compute α_{sdb} for simplex b since a negative f_0 implies that the pot composition would have to travel backwards to intersect $\hat{\mathbf{\Pi}}_b^2$.

The general procedure goes as follows: let $x_{m_a}^*$ and $x_{m_b}^*$ represent the two unstable nodes in the system, and let $x^{p,0}$ represent the initial composition. $\alpha_{\text{sdb}}^{m_i}$ represents the relative distance from the initial composition to the stable dividing boundary, and $\alpha_{\text{pps}}^{m_i}$ represents the relative distance from the initial composition to the product simplex boundary of a pos-

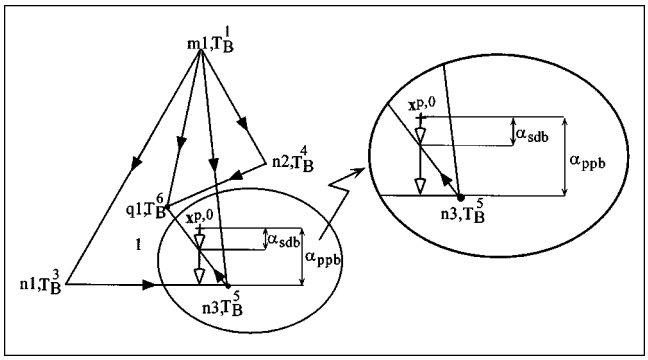

Figure 9. Calculation of relative distance from initial composition to intersection.

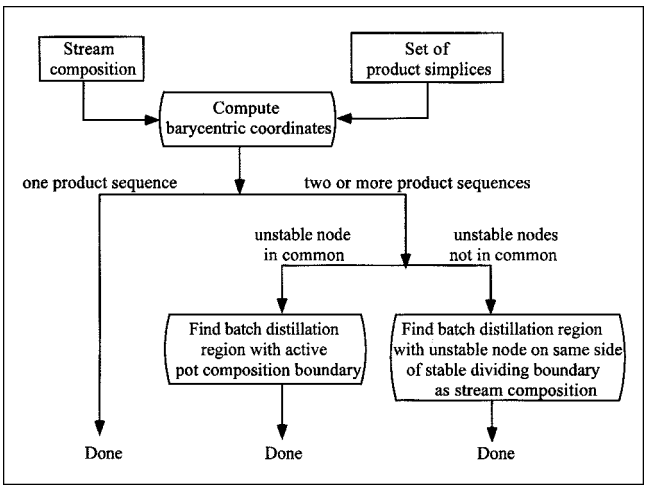

Figure 10. Strategy for predicting correct product sequence.

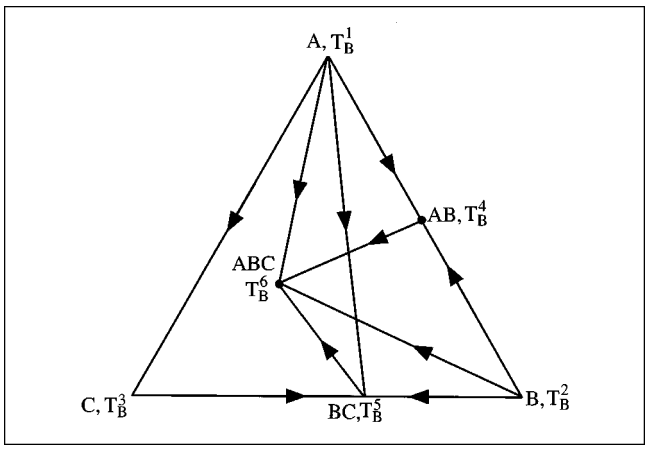

Figure 11. Composition simplex with batch distillation regions for the ternary system.

itive product simplex. The superscript m_i refers to unstable node m_i. The fixed points on the stable dividing boundaries are the points in $\overline{\omega}^{uc}$ $(x^*_{m_a,\ x^*m_b})$, the common unstable boundary limit set (which can be extracted from the boundary limit sets constructed by the algorithm of Ahmad et al. (1998)).

(1) Dividing $\overline{\omega}^{uc}$ $(x^*_{m_a}, x^*_{m_b})$ into sets of $nc-1$ points which each define a product simplex boundary. The product simplex boundaries will be used to approximate the stable dividing boundary.

(2) For each unstable node:

(a) Construct sets of nc points by combining the unstable node with each of the sets of $nc-1$ points. Each set of nc points define an $(nc-1)$-simplex.

(b) For all the simplices (both the positive product simplex and the new simplices), compute the barycentric coordinates by applying Eqs. 2 to $x^{p,0}$.

(c) Finally, compute $\alpha^{m_i}_{\text{sdb}}$ and $\alpha^{m_i}_{\text{ppb}}$ using Eq. 5. Alternatively, apply Eq. 6, where s now is the set of simplices (both the original positive product simplex and the new simplices) containing the same unstable node and which have positive barycentric coordinates.

(d) If any $\alpha^{m_i}_{\text{sdb}} < \alpha^{m_i}_{\text{ppb}}$, then $x^{p,0}$ is not in the batch distillation region giving rise to $x^*_{m_i}$ in the first cut.

The overall strategy for predicting the correct product sequence is summarized in Figure 10.

Calculating Maximum Recovery

Once the correct product sequence has been found, the fractions of the initial mixed-solvent stream recovered in each cut must be calculated. Of course, if some of the species are very close boiling, we may not be able to achieve good separation no matter how many trays the column has, and no matter how high reflux ratio the column operates at. However, for the purpose of this work, we assume that sharp splits are always obtained. This will give us the theoretical maximum flows and, hence, targeting.

The amounts recovered in each cut can be computed by solving a simple material balance for each of the components present

$$F^{p,0} = \sum_{k=0}^{nc-1} F_k p_k; \quad F_k \geq 0 \ \forall k = 0, \ldots, nc-1 \qquad (7)$$

$F_i^{p,0}$ is the total number of component i initially in the reboiler, and F_k is the total number of moles recovered in product cut k. The material balance confirms that $\sum_{k=0}^{nc-1} F_k = \sum_{i=1}^{nc} F_i^{p,0} = F^{p,0}$. Hence, we have nc equations and a set of nc unknowns $(F_0, F_1, \ldots, F_{nc-1})$, and the system is therefore fully defined. Division by $F^{p,0}$ results in equations similar to form to Eq. 2. The recovered fractions are in fact the barycentric coordinates f_k $\forall k = 0, \ldots, nc-1$ already computed for locating the feed composition.

Ternary Example

The presented procedures for locating a stream composition and computing maximum recovery were applied to several ternary mixtures involving the same three components. The composition simplex with the batch distillation regions is shown in Figure 11, the composition of the fixed points in the ternary system can be found in Table 2, and the unstable boundary limit sets are listed in Table 3. The four product sequences in the system are listed in Table 4.

Three different stream compositions were tested: $x_1^{p,0} = [0.2, 0.2, 0.6]^T$, $x_2^{p,0} = [0.5, 0.2, 0.3]^T$, and $x_3^{p,0} = [0.2, 0.4, 0.4]^T$. The barycentric coordinates were computed for each compo-

Table 2. Fixed Points in Ternary System

e	A	B	C
A	1	0	0
B	0	1	0
C	0	0	1
AB	0.5	0.5	0
BC	0	0.6	0.4
ABC	0.3	0.2	0.5

Table 3. Unstable Boundary Limit Sets

e	$\overline{\omega}^u(x_e^*)$
A	C, AB, BC, ABC
B	AB, BC, ABC
C	BC
AB	ABC
BC	ABC
ABC	$\emptyset$

Table 4. Product Sequences in Ternary System

b	Product Sequence
1	{A, C, BC}
2	{A, AB, ABC}
3	{B, AB, ABC}
4	{B, BC, ABC}

sition point by applying Eq. 2 to the four constructed product simplices ($\mathbf{\Pi}_1^3$, $\mathbf{\Pi}_2^3$, $\mathbf{\Pi}_3^3$ and $\mathbf{\Pi}_4^3$). The values are listed in Table 5.

Composition point $x_1^{p,0}$ results in positive barycentric coordinates for product simplex $\mathbf{\Pi}_1^3$ only. Hence, the correct product sequence is $P_1 = \{A, C, BC\}$. The amounts recovered in each product cut can be extracted directly from Table 5. f_A is equal to 0.2, f_{BC} is equal to 0.47, and f_{BC} is equal to 0.33.

Composition point $x_2^{p,0}$ results in positive barycentric coordinates for both product simplex $\mathbf{\Pi}_1^3$ and $\mathbf{\Pi}_2^3$. The respective product sequences share the same unstable node (A). We therefore need to determine which batch distillation region (B_1 or B_2) contains the active batch distillation boundary.

The relative distance to the boundary may be computed using Eq. 5. Alternatively, Eq. 6 may be applied directly to the barycentric coordinates for the first product cut. From Table 5, we find that $f_A^1 = 0.5$, while $f_A^2 = 0.24$. Consequently, batch distillation region 2 contains the active batch distillation boundary, and $x_2^{p,0}$ will give rise to product sequence $P_2 = \{A, AB, ABC\}$. The fractions recovered of each product cut can be extracted directly from Table 5. f_A is equal to 0.24, f_{AB} is equal to 0.16, and f_{ABC} is equal to 0.6.

Composition point $x_3^{p,0}$ results in positive barycentric coordinates for both product simplex $\mathbf{\Pi}_1^3$ and $\mathbf{\Pi}_4^3$. The respective product sequences do not share the same unstable node. Product sequence P_1 has pure component A as its first product cut, while product sequence P_4 has pure component B as its first product cut. We therefore need to determine which batch distillation region (B_1 or B_4) has the unstable node on the same side of the stable dividing boundary as stream composition $x_3^{p,0}$. This is done by performing the steps in the previous section.

The common unstable boundary limit set is determined from Table 3 (Ahmad et al., 1998)

$$\overline{\omega}^{uc}(A, B) = \{C, AB, BC, ABC\} \cap \{AB, BC, ABC\} = \{AB, BC, ABC\} \quad (8)$$

The stable dividing boundary is approximated by the two product simplex boundaries $\hat{\mathbf{\Pi}}_2^2$ defined by $\hat{P}_2 = \{AB, ABC\}$, and $\hat{\mathbf{\Pi}}_4^2$ defined by $\hat{P}_4 = \{BC, ABC\}$. First, two new 2-simplices are generated by adding A as the first vertex, defined by the vertices $S_a = \{A, AB, ABC\}$, and $S_b = \{A, BC, ABC\}$. The barycentric coordinates are computed for these new simplices for $x_3^{p,0}$. The values are shown in Table 6.

Simplex a has some negative barycentric coordinates. We therefore only need to compute the relative distances $\alpha_{\text{sdb},b}^A$ and α_{ppb}^A. This is done by applying Eq. 5

$$\alpha_{\text{sdb},b}^A = \frac{1}{1-0.091} = 1.1 \quad (9)$$

$$\alpha_{\text{ppb}}^A = \frac{1}{1-0.2} = 1.25 \quad (10)$$

$\alpha_{\text{sdb},b}^A < \alpha_{\text{ppb}}^A$. Hence, $x_3^{p,0}$ is not located in batch distillation region 1. Consequently, it must be located in batch distillation region 4. For completeness, the procedure is repeated for unstable node B.

Two new 2-simplices are generated by adding unstable node B as the first vertex, defined by the vertices $S_c = [B, AB, ABC\}$, and $S_d = \{B, BC, ABC\}$. The barycentric coordinates are computed for these new simplices for $x_3^{p,0}$. The values are shown in Table 7.

Simplex c has some negative barycentric coordinates. We therefore only need to compute the relative distances $\alpha_{\text{sdb},d}^B$ and α_{ppb}^B. This is done by applying Eq. 5

Table 5. Barycentric Coordinates

	$\mathbf{\Pi}_1^3$			$\mathbf{\Pi}_2^3$			$\mathbf{\Pi}_3^3$			$\mathbf{\Pi}_4^3$		
	f_A	f_C	f_{BC}	f_A	f_{AB}	f_{ABC}	f_B	f_{AB}	f_{ABC}	f_B	f_{BC}	f_{ABC}
$x_1^{p,0}$	0.2	0.47	0.33	−0.12	−0.08	1.2	0.12	−0.32	1.2	−0.11	0.44	0.67
$x_2^{p,0}$	0.5	0.17	0.33	0.24	0.16	0.6	−0.24	0.64	0.6	0.22	−0.89	1.67
$x_3^{p,0}$	0.2	0.13	0.67	−0.28	0.48	0.8	0.28	−0.08	0.8	0.22	0.11	0.67

Table 6. Barycentric Coordinates for $x_3^{p,0}$

	$\mathbf{\Pi}_1^3$			Simplex a			Simplex b		
	f_A	f_C	f_{BC}	f_A	f_{AB}	f_{ABC}	f_A	f_{BC}	f_{ABC}
$x_3^{p,0}$	0.2	0.13	0.67	−0.28	0.48	0.8	0.091	0.55	0.36

Table 7. Barycentric Coordinates for $x_3^{p,0}$

	$\mathbf{\Pi}_4^3$			Simplex c			Simplex d		
	f_B	f_{BC}	f_{ABC}	f_B	f_{AB}	f_{ABC}	f_B	f_{BC}	f_{ABC}
$x_3^{p,0}$	0.22	0.11	0.67	0.28	−0.08	0.8	0.22	0.11	0.67

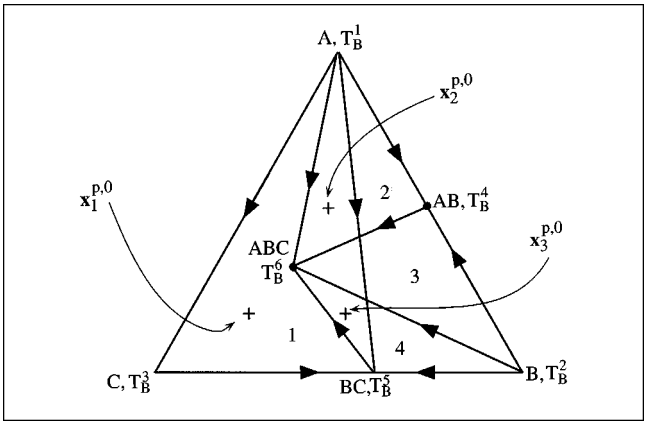

Figure 12. Locations of the composition points in the composition simplex.

$$\alpha^{B}_{\text{sdb},\,d} = \frac{1}{1-0.22} = 1.28 \tag{11}$$

$$\alpha^{B}_{\text{ppb}} = \frac{1}{1-0.22} = 1.28 \tag{12}$$

so that $\alpha^{B}_{\text{sdb},\,d} = \alpha^{B}_{\text{ppb}}$. Hence, the result above is confirmed. The fractions recovered in each product cut can be extracted directly from Table 5. f_B is equal to 0.22, f_{BC} is equal to 0.11, and f_{ABC} is equal to 0.67. For clarity, the locations of the composition points in the composition simplex are shown in Figure 12.

Example: Siloxane Monomer Process

Base case

Solvent recovery targeting is applied to the production of a siloxane based monomer in a single campaign (Figure 13). The process consists of several sequential reaction steps. Solvents and reaction by-products are separated from products through batch distillation. Further details concerning the process can be found in Allgor et al. (1996). The different unit operations were simulated using ABACUSS [ABACUSS (Advanced Batch and Continuous Unsteady-State Simulator) Process Modeling Software, a derivative work of gPROMS Software)]. The azeotropic behavior was approximated using the Wilson model to calculate the activity coefficients [see, for example, Reid et al. (1987)]. Binary parameters were extracted from Aspen Plus (Aspen Technology, 1995). Missing binary parameters were estimated using the UNIFAC group contribution method (Fredenslund et al., 1977) as implemented in Aspen Plus (Aspen Technology, 1995). Binary parameters for the pairs involving the nonstandard components R2, C, E, A, and D can be found in Ahmad (1997). R1 represents allyl alcohol. The vapor phase was assumed to be ideal. A batch size of 780 kg of product (A + D) was used as a basis for the simulations.

There are two mixed waste-solvent streams generated in the process. Firstly, the stream leaving overhead from the first rectifier contains large amounts of toluene (T) and methanol (M), about 23% of the reactant R1, and small amounts of the intermediate E. The composition simplex for this system divided into batch distillation regions is presented in Figure 14. E is not included as there is very little of this intermediate present in the stream. Also, E does not form an azeotrope with any of the other components. The mixture exhibits a low-boiling binary azeotrope between methanol and toluene (M-T), and a low-boiling binary azeotrope between toluene and R1 (R1-T). There are three batch distillation regions present, each resulting in different product sequences with three cuts: $P_1 = \{\text{M-T, M, R1}\}$, $P_2 = \{\text{M-T, R1-T, R1}\}$, and $P_3 = \{\text{M-T, R1-T, T}\}$. In this case the generated product simplices coincide with their respective batch regions. The initial composition places the stream in region 3. At the limit, 28% or about 2.4 kmol will be recovered as the methanol-toluene azeotrope, 34% or about 2.95 kmol as the R1-toluene azeotrope, and 38% or 3.3 kmol as pure toluene. Hence, only toluene can possibly be recovered as a pure component. Provided that the fraction of methanol in the R1-toluene cut is very small, this cut could probably be recycled back to reaction step I. To avoid premature reaction of C with methanol,

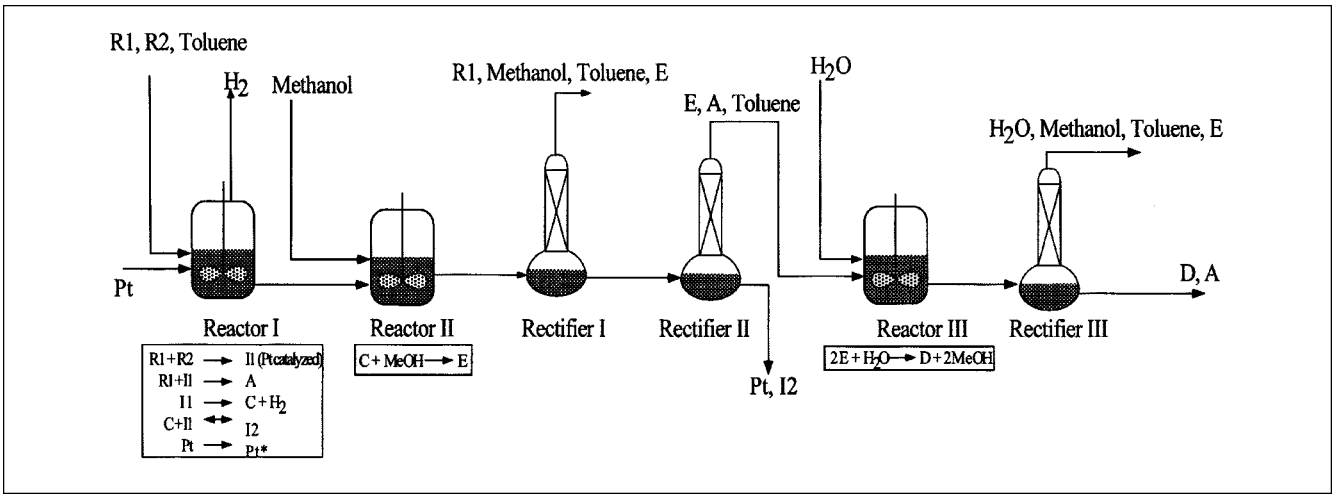

Figure 13. Siloxane monomer process: base case.

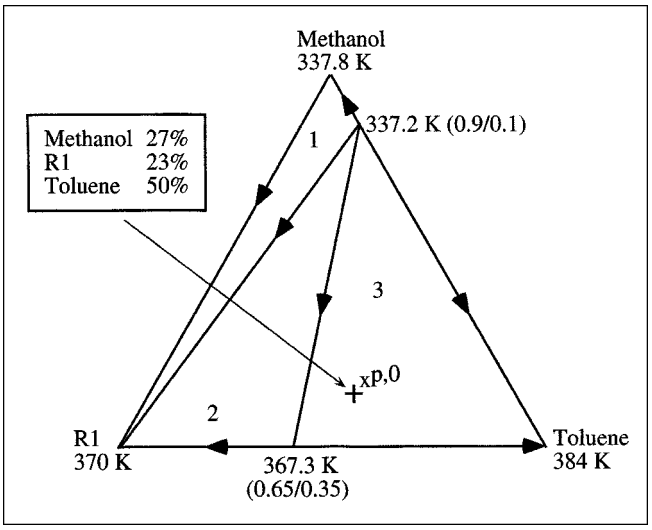

Figure 14. Composition simplex for the system methanol, R1, and toluene at 1 atmosphere.

methanol may not enter reaction step I. In addition, recycling of the methanol-toluene azeotrope to reaction step II will result in unacceptable buildup of toluene. Therefore, at least 28% of this stream (the methanol-toluene azeotrope) could not be recovered. In other words, at least 28% of the stream would end up as organic waste.

Secondly, the aqueous stream leaving overhead from rectifier III contains about 95% water, and traces of toluene, methanol (formed in reaction step III), and intermediate E. It is assumed that the organic compounds would end up as organic waste. The stream is heterogeneous, forming a water-rich liquid phase and a toluene-rich liquid phase. The components also form three binary azeotropes, one between methanol and toluene, one between water and toluene, and one between water and E. The majority of the toulene and E could be removed in a decanter, while most of the remaining methanol in the aqueous phase could be removed through distillation. The estimated amount of organic waste from this stream is about 170 kg per batch, and the total amount of organic waste from the two mixed waste-solvent streams is 282 kg or about 5 kmol. Can we do better?

Process alternative

By studying the composition simplices created for all the process streams, several process alternatives were generated. Only the most promising one will be discussed here, but it should be noted that there are other acceptable solutions.

Toluene and intermediate E are relatively narrow boiling, and it is therefore difficult to achieve a sharp split between these two components. Hence, in order to avoid loss of intermediate E, a large fraction of toluene is left in the reboiler at the end of distillation I, and, consequently, toluene will remain with the product and will not be removed until distillation III. This complicates solvent recovery since toluene forms a binary azeotrope with methanol. It was therefore proposed to introduce a batch distillation column between reaction step I and II as indicated in Figure 15. Three product cuts were proposed. Intermediate C is recovered for reaction step II, toluene and excess reactants are recycled back to reaction step I, and product A is purified. Methanol and C are recovered in rectifier II, and recycled directly back to reactor II. No toluene is carried through to the last column. The aqueous waste stream is therefore only contaminated with methanol which will greatly simplify the cleanup of the stream. The stream composition is about 45 kmol water and 1.3 kmol methanol. All the toluene is recovered and recycled, and there will be no toluene losses from the process. In fact, since the excess methanol from reaction step II is recycled, only the methanol generated in reaction step III (1.3 kmol) and removed in a water treatment facility will appear as organic waste. The total amount of organic waste is reduced by approximately 70% compared to the base case. Other improvements are also achieved: raw material is saved, and the load on downstream units is reduced.

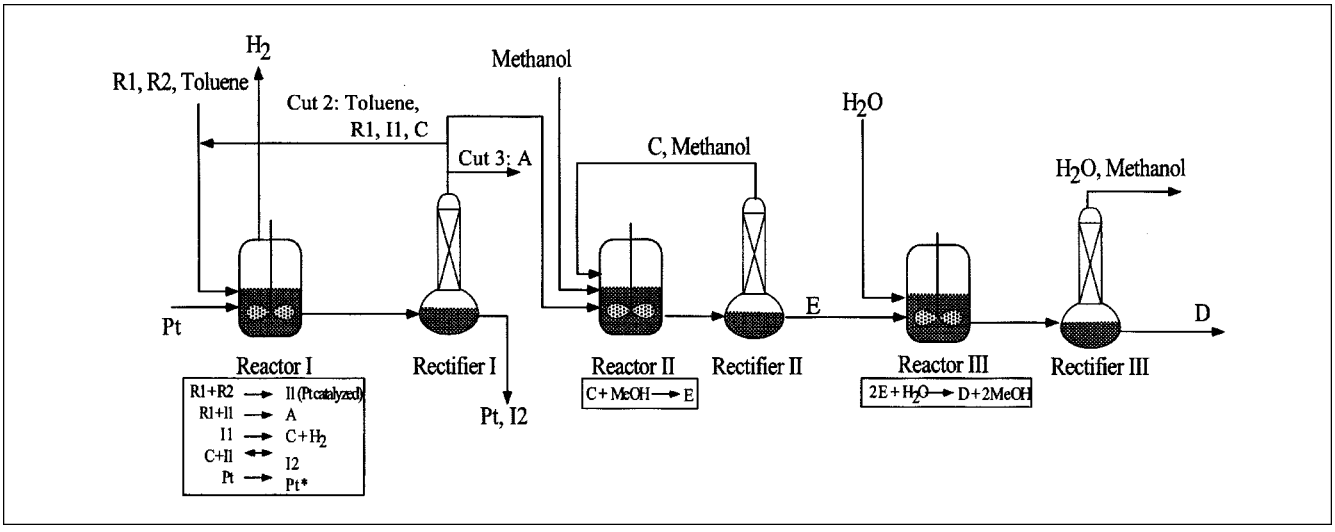

Figure 15. Process alternative.

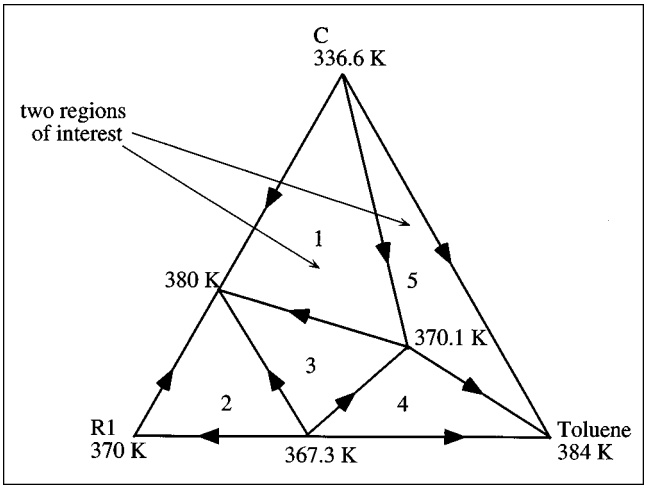

Figure 16. Residue curve map for the system toluene, R1, and C at 1 atmosphere.

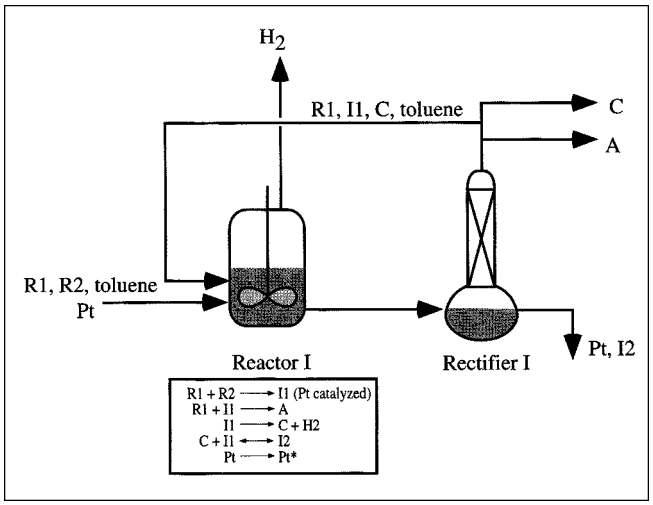

Figure 17. Model of coupled reactor and distillation column.

An analysis of the new composition simplex for the ternary system C, R1, and toluene using solvent recovery targeting indicates that there are two batch distillation regions from which intermediate C can be recovered as a pure species (see Figure 16).

However, C forms a binary azeotrope with R1 and a ternary azeotrope with R1 and toluene, Hence, while C can be recovered as a pure species, a large fraction of C will also be recycled back to reaction step I. Recycling of C will lead to buildup of C in the reactor to a *cyclic steady-state* concentration (a cyclic dynamic system is said to have reached cyclic steady-state when the variable profiles over a cycle are the same from one cycle to the next). A reversible reaction with C forms the undesired oligmer I2, and recycling of C will encourage formation of I2. Consequently, while solvent recovery targeting has determined that the proposed process modification is indeed feasible, it may not be acceptable as it could possibly lower the selectivity of A over C and increase the formation of undesired byproducts. A more detailed analysis of the effects of recycling C on the chemistry in reaction step I is essential. A feasibility study of the coupled system consisting of Reactor I, Rectifier I, and the recycle stream was therefore performed.

Dynamic modeling of coupled reactor and distillation column

As a result of the solvent recovery targeting analysis, several design objectives were identified for the detailed feasibility study:

- The mixture leaving reaction step I at cyclic steady state must be in either batch distillation region 1 to 5 to allow recovery of pure C, and, hence, feasibility of the process modification.
- The overall operating policy must aim to minimize formation of the undesired oligmer I2.
- It must be possible to design a startup policy that will take the coupled system to the desired cyclic steady-state in a reasonable number of cycles.

The key design variables are the charge and temperature policies for the reactor (which will control the amount of solvent, reagent and C in the feed to the column, and the concentration of I1, and, hence, I2), and the reflux policy and accumulator dumps for the column. Also, we are concerned with designing not only the optimal cyclic steady-state policy, but also a startup policy to take a cold and empty system to this cyclic steady state.

Preliminary feasibility of the overall mass balance (that is, can the system operate in one of the target distillation regions) can be verified via a MILP (mixed integer linear program) formulation of the mass balances and batch distillation regions (Ahmad and Barton, 1995). However, a dynamic study is required to address all the issues raised above in detail. Therefore, a dynamic model of the coupled reactor and the column system was created (see Figure 17). The coupled reactor-distillation system was modeled using ABACUSS, applying the same unit operation models as in the base case calculations. Only the operating policies and connectivity of the flowsheet were modified.

The first step was to establish feasibility of startup through the use of dynamic simulation studies to design interactively a startup sequence that can take the system to a cyclic steady state operating in one of the target batch distillation regions. The SCHEDULE features of ABACUSS (Barton, 1992; Barton and Pantelides, 1994), which allow modeling of complex sequences of control actions, were particularly useful here to formulate and experiment with alternative sequences. After some experimentation, a feasible startup sequence was found as follows:

- Charge all of the R1 and toluene initially.
- Heat the reaction mass to its boiling temperature and then turn the steam to the heating jacket turn off.
- Add the catalyst slurry.
- Over the next two hours, charge R2 continuously to maintain a high concentration of R1 relative to that of R2 (this feed policy favors formation of A over C).

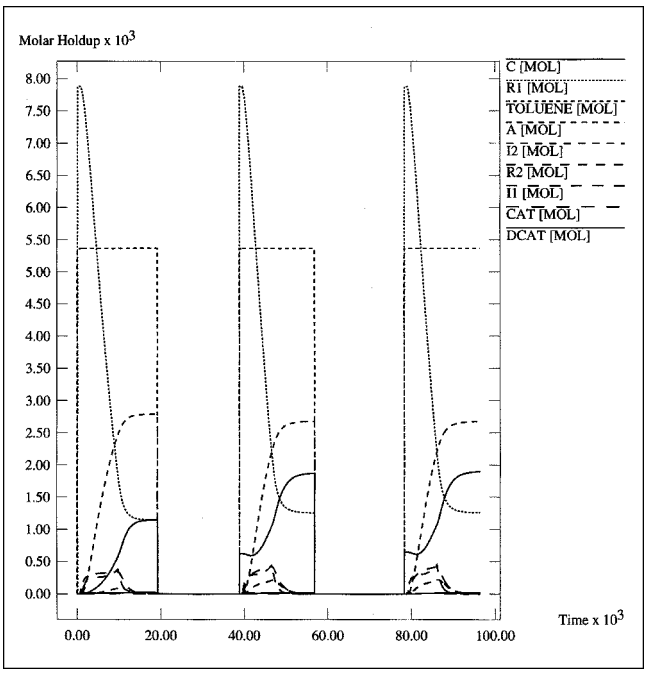

Figure 18. Holdup in reaction step I over three cycles.

• Allow the reaction to continue until the amount of R1 or R2 was less then 0.1 mol, then discharge the reactor to intermediate storage awaiting separation.

Similarly, the operating policy for the column splits the feed into the sequence of cuts shown in Figure 17. These cycles are then repeated, except that in subsequent cycles the second distillation cut (consisting of R1, toluene, and C and small amounts of I1, R2, and A) is recycled from the distillation column to form part of the reactor charge. This recycle stream significantly decreases the amount of fresh R1 and toluene needed.

According to this policy, the composition profile in reaction step I reaches cyclic steady state after four cycles. Only a slight increase in the formation of C was observed, while the formation of A consequently reduced a similar amount. No noticeable increase in the formation of I2 was detected, and startup leading to a cyclic steady state in one of the target batch distillation regions is feasible. The holdup profiles in reaction I over the first three cycles are plotted in Figure 18.

The optimal cyclic steady-state operating policy can be determined using the detailed dynamic model and the dynamic optimization features of ABACUSS (Feehery and Barton, 1998; Allgor, 1997). According to the approach developed by Charalambides (1996), the composition and temperature of the intermediate storage between two units at cyclic steady state can be represented as time invariant parameters in a dynamic optimization formulation that can solve directly for the optimal cyclic steady-state policy (that is, without the need to simulate multiple cycles until cyclic steady state is reached). This formulation simultaneously determines optimal charge and temperature profiles for the reactor, and reflux profiles, and dumping and recycle policies for the column to, for example, maximize yield of A and C, or minimize raw material and operating costs. In fact, the results of the simulation study above are very important in providing initial guesses, particularly for the intermediate storage compositions that start the optimization in a batch distillation region that yields a feasible cyclic steady state. However, it should be noted that currently the model used by the dynamic optimization calculations must be simplified relative to the model used for the simulation studies in order to remove phenomena such as boiling in the reactor, because the algorithms employed cannot deal with implicit discontinuities (or state events (Park and Barton, 1996)) in the model.

As can be seen from this study, a detailed dynamic model of the coupled reactor and distillation column used in conjunction with solvent recovery targeting was extremely valuable in designing integrated operating policies for the reaction and distillation tasks to minimize the formation of I2, and also to ensure feasibility in the sense that the mixture to be separated is placed in a batch distillation region from which C can be recovered as a pure species. As this type of modeling technology becomes increasingly available in industry, it will offer a cheaper, safer, quicker and more effectie alternative to explore different operating policies than more conventional pilot-scale studies.

Example: Production of a Carbinol

Solvent recovery targeting was applied to a process for the production of a carbinol (5-methyl-5H-dibenzo[a,d]cycloheptene-5-ol) (see Figure 19). The synthesis represents one of the 10 steps in a manufacturing process for the production of

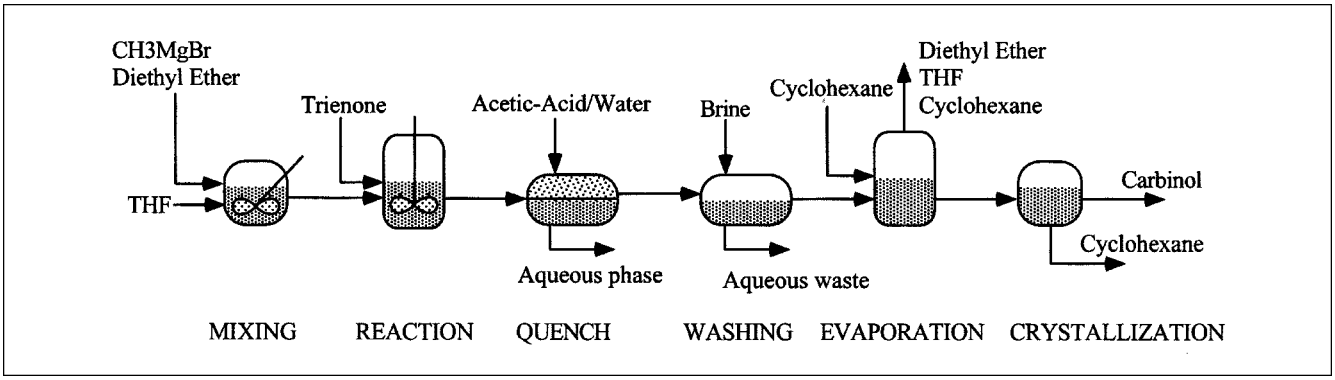

Figure 19. Flowsheet for production of a carbinol.

5-methyl-10,11-dihydro-5H-dibenzo[a,d]cycloheptene-5,10,imine,maleate.

The process consists of a reaction step followed by quenching with an aqueous solution and a two-phase separation, and washing with brine. Then, the reaction solvent is replaced by the crystallization medium through evaporation, and the product is crystallized and collected through filtration. In the reaction step trienone is converted to carbinol. A major impurity is tetraene, produced by acid catalyzed elimination of carbinol. Further details about the process can be found in Aumond (1994) and Linninger et al. (1994). The azeotropic behavior was approximated using the Nonrandom-Two-Liquid (NRTL) model (Renon and Prausnitz, 1968) to calculate the activity coefficients. Binary parameters were extracted from Aspen Plus (Aspen Technology, 1995). A batch size of 500 kg of carbinol was used as basis for the study.

The major organic waste stream results from the replacement of the reaction medium tetrahydrofuran (THF) with crystallization medium cyclohexane. The solvent switch takes place through evaporation, and the resulting waste stream is a ternary mixture consisting of about 12.1 kmol of diethyl ether (10%), 40.4 kmol of THF (33.3%), and 68.8 kmol of cyclohexane (56.7%). It is desirable to recover the solvents for reuse through batch distillation. The composition simplex for this mixture at 1 atmosphere is shown in Figure 20. Cyclohexane and THF exhibit a low-boiling binary azeotrope. Varying the pressure reveals that the azeotrope is not very pressure sensitive. Running the separation at lower pressure therefore does not provide any significant benefits. The pure component diethyl ether is the only unstable node, and the two batch distillation regins will both give rise to diethyl ether as the first product, followed by the binary azeotrope. Depending on the location of the initial composition, the final cut will be either pure cyclohexane or pure tetrahydrofuran. The initial composition places the mixed waste-solvent stream in region 1, and therefore diethyl ether (12.1 kmol) and cyclohexane (65.52 kmol) can be recovered as pure components and reused, while THF will be recovered as part of the azeotrope (43.68 kmol). Since cyclohexane is the crystallization medium, recycling the recovered binary azeotrope to the reactor may cause some of the product to crystallize prematurely. The fraction of cyclohexane in the azeotrope is relatively small and may not cause a problem. However, if premature crystallization is not acceptable, the binary azeotrope has to be disposed of or possibly be split using an entrainer, an alternative that is not considered here. In that case, the base will result in at least 43 kmol or about 3,190 kg of organic waste per batch. Moving the composition of the mixed waste-solvent stream to region 2 by adding tetrahydrofuran and achieving recovery of pure THF would result in the same problem, as recovery of the azeotrope cannot be avoided. In addition, the binary azeotrope and THF are very close boiling, making it almost infeasible to obtain a sharp split.

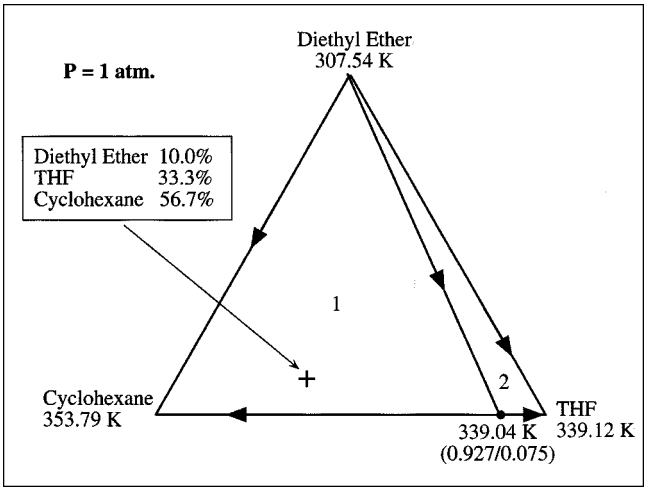

Figure 20. Composition simplex for the system diethyl ether, tetrahydrofuran, and cyclohexane.

The most promising option for process improvement lies in replacing THF with a solvent that allows for easier recovery. It is also advantageous to replace THF, because it is miscible with water at atmospheric conditions (Wisniak, 1980), and solvent is often lost to the aqueous phase. Other problems associated with THF include its extreme flammability and the potential for formation of peroxides (Molnar, 1996). Several issues have to be kept in mind when evaluating alternative solvents:

(1) It must be compatible with the process chemistry.

(2) It should preferably be completely or partially immiscible with water to facilitate a two-phase split to remove salts from the organic phase.

(3) It should preferably be less harmful the replaced solvent, THF.

The reaction is a Grignard addition. Ethers are usually employed as Grignard reaction media, due to the ether group that is attracted by the highly electrophilic magnesium atom in the Grignard compound. An obvious choice in this case is to employ diethyl ether since it is already used as storage medium for the Grignard compound. Diethyl ether is also suggested by Reichardt (1988) as a common solvent for Grignard reactions. Diethyl ether is partially immiscible with water (Wisniak, 1980) and will form the organic rich phase following the two-phase split. Furthermore, the replacement of cyclohexane through evaporation will result in a binary solvent waste stream of diethyl ether and cyclohexane. Returning to the composition simplex in Figure 20 reveals that diethyl ether can be easily separated from cyclohexane, resulting in complete recovery of solvents. However, it is expected that the use of diethyl ether will reduce the reaction rate, as the nucelophilic ether group in diethyl ether may not be as efficient as in THF due to the molecule's linear structure. Laboratory experiments are necessary to resolve this issue.

Another possibility is to replace THF with a novel solvent replacement. For example, Molnar (1996) designs and synthesize a new class of solvents having similar properties to THF, but which are nonvolatile and can be easily recovered from process streams using simple mechanical separation operations such as ultrafiltration. The polymer solvent system is generated by attaching THF to a polymer backbone and dissolving it in a relatively benign continous phase. In the example process the polymer based solvent can be recovered from the organic product stream after the washing operation, leaving the product (carbinol) dissolved in the inert solvent. The inert solvent is then replaced by cyclohexane through evapo-

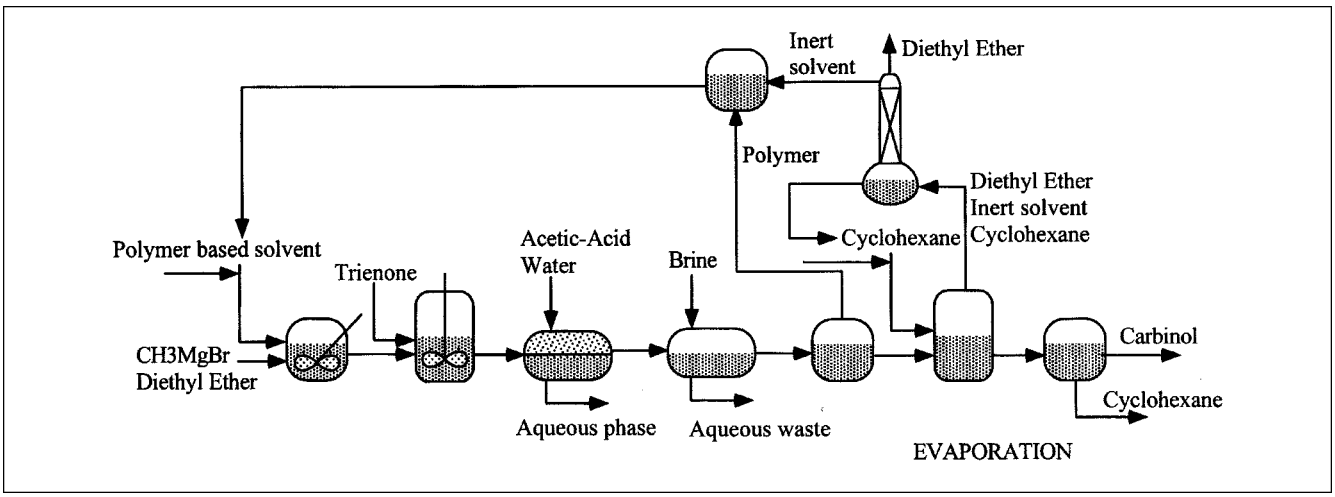

Figure 21. Improved process flowsheet.

ration as in the base case. Thus, we are again left with a mixed solvent-waste stream consisting of diethyl ether, cyclohexane, and the inert solvent that needs to be analyzed. Molnar (1996) tests different compositions of mixtures of toluene, hexane, and heptane as candidates for the inert continuous phase. Liquid-liquid phase diagrams in Wisniak (1980) show that these three components are all almost completely immiscible in water. Applying solvent recovery targeting discloses that none of the components form azeotropes with diethyl ether or cyclohexane. Consequently, separating the solvent-waste mixture through batch distillation would be relatively easy, and again no unnecessary organic waste is generated. Laboratory experiments should be preformed to determine which of the candidate solvents (or mixture of) would result in the optimal reaction conditions. The resulting flowsheet indicating solvent recovery and recycling is shown in Figure 21.

Conclusions

A recently reported algorithm (Ahmad et al., 1998) for characterizing the batch distillation composition simplex for a system with an arbitrary number of components was exploited to develop a sequential design strategy in which process streams or mixed waste-solvent streams are analyzed for maximum feasible solvent recovery. This procedure is termed *solvent recovery targeting*. For a given base case, solvent recovery targeting will, given the composition of the mixture(s) to be separated, predict the correct distillation sequence and calculate maximum feasible recovery of each product cut in the sequence. It can further provide information about all other feasible distillation sequences involving the same set of pure components. The information is used to evaluate the feasibility of enhancing solvent recovery in the proposed flowsheet, and to guide the improvement of a flowsheet with respect to solvent recovery.

Solvent recovery targeting was applied to two case studies. The first case study involves a siloxane monomer process. By using the targeting algorithm to explore the feasible separation alternatives, it was found that a reduction of about 70% in the organic waste compared to the base case could be achieved by integrating solvent recovery and recycling into the flowsheet. Also, it was demonstrated how a dynamic simulation model can be exploited to evaluate the proposed process alternative with respect to effects on the reaction chemistry when an intermediate is recycled. The model yields insights for the design of integrated operating policies that increase yield and selectivity and minimize formation of an undesired byproduct.

Similarly, in a second case study involving the manufacture of a carbinol, solvent recovery targeting was used to evaluate several possible process modifications to improve solvent recovery. In particular, replacing the original solvent THF with a novel polymer based solvent proved very promising.

Acknowledgments

This research was supported by the Emission Reduction Research Center under grant E12 9/96760, and the Chlorine Project of the MIT Initiative in Environmental Leadership. The authors would like to thank Sarwat Khattak for performing the dynamic simulations for the Siloxane Monomer case study.

Literature Cited

Ahmad, B. S., and P. I. Barton, "Synthesis of Batch Processes with Integrated Solvent Recovery and Recycling," Paper No. 187d, AIChE Meeting (Nov. 1995).

Ahmad, B. S., and P. I. Barton, "Homogeneous Multicomponent Azeotropic Batch Distillation," *AIChE J.*, **42**, 3419 (1996).

Ahmad, B. S., Y. Zhang, and P. I. Barton, "Product Sequences in Azeotropic Batch Distillation," *AIChE J.*, **44**, 1051 (1998).

Ahmad, B. S., "Synthesis of Batch Processes with Integrated Solvent Recovery," PhD Thesis, Massachusetts Institute of Technology (1997).

Allgor, R. J., M. D. Barrera, P. I. Barton, and L. B. Evans, "Optimal Batch Process Development," *Comput. Chem. Eng.*, **20**, 885 (1996).

Allgor, R. J., "Modeling and Computational Issues in the Development of Batch Processes," *PhD Thesis, Massachusetts Institute of Technology* (1997).

Aspen Technology, *ASPEN PLUS User Manual Release 9*, Aspen Technology Inc., Cambridge, MA (1995).

Aumond, J. P, ''Plant-Wide Solvent Identification for Pharmaceutical and Fine Chemical Processes,'' Technical Report, Doctoral Thesis Proposal, Mass. Inst. of Technol. (1994).
Barton, P. I., and C. C. Pantelides, ''Modeling of Combined Discrete/Continuous Processes,'' *AIChE J.*, **40**(6), 966 (1994).
Barton, P. I., ''The Modeling and Simulation of Combined Discrete/Continuous Processes,'' PhD Thesis, Univ. of London (1992).
Chadha, N., and C. S. Parmele, ''Minimize Emissions of Air Toxics via Process Changes,'' *Chem. Eng. Prog.*, 37 (Jan., 1993).
Charalambides, M. S., ''Optimal Design of Integrated Batch Processes,'' PhD Thesis, Univ. of London (1996).
Feehery, W. F., and P. I. Barton, ''Dynamic Optimization with State Variable Path Constraints,'' *Computers Chem. Eng.*, **22**, 241 (1998).
Fredenslund, Aa., J. Gmehling, and P. Rasmussen, *Vapor-Liquid Equilibria using UNIFAC*, Elsevier, Amsterdam (1977).
Freeman, H., T. Harten, J. Springen, P. Randall, M. A. Currant, and K. Stone, ''Industrial Pollution Prevention: A Critical Review,'' *J. for Air and Waste Manage. Assoc.*, **42**, 618 (1992).
Hassan, S. Q., and D. L. Timberlake, ''Steam Stripping and Batch Distillation for the Removal and/or Recovery of Volatile Organic Compounds from Industrial Waste,'' *Air Waste Manage. Assoc.*, **42**, 936 (1992).
Heckman, R. A., ''Alternatives for Hazardous Industrial Solvents and Cleaning Agents,'' *Pollut. Prev. Rev.* (Summer, 1991).
Kirschner, E. M., ''Environment, Health Concerns Force Shift in Use of Organic Solvents,'' *Chem. Eng. News*, 13 (June 20, 1994).
Linninger, A. A., S. A. Ali, E. Stephanopoulos, C. Han, and G. Stephanopoulos, ''Synthesis and Assessment of Batch Processes for Pollution Prevention,'' *AICHE Symp. Ser.*, **90**(303), 46 (1994).
Molnar, L. K., ''Polymer-Based Solvent for Minimizing Pollution During the Synthesis of Fine Chemicals,'' PhD Thesis, Massachusetts Institute of Technology (1996).
Park, T., and P. I. Barton, ''State Event Location in Differential-Algebraic Models,'' *ACM Trans. Mod. and Comput. Sim.*, **6**(2), 137 (1996).
Reichardt, C., *Solvents and Solvent Effects in Organic Chemistry*, 2nd ed., VCH Verlagsgesellschaft mbH, Germany (1988).
Reid, R. C., J. M. Prausnitz, and B. E. Poling, *The Properties of Gases and Liquids*, 4th ed., McGraw-Hill, New York (1987).
Renon, H., and J. M. Prausnitz, ''Local Compositions in Thermodynamic Excess Functions for Liquid Mixtures,'' *AIChE J.*, **14**, 135 (1968).
Van Dongen, D. B., and M. F. Doherty, ''On the Dynamics of Distillation Processes: VI. Batch Distillation,'' *Chem. Eng. Sci.*, **40**, 2087 (1985).
Wisniak, J., *Liquid-Liquid Equilibrium and Extraction: A Literature Source Book, V.1.*, Elsevier Scientific Pub. (1980).

Manuscript received May 26, 1998, and revision received Nov. 24, 1998.